Proceedings of Nuclear and Emerging Technologies for Space 2013
Albuquerque, NM, February 25-28, 2013
Paper xxxx

Design of a Uranium Dioxide Spheroidization System

Daniel P. Cavender[1], Omar R. Mireles[1], Abdelkader Frendi[2]

[1]*NASA Marshall Space Flight Center, Huntsville AL 35812*

[2]*University of Alabama-Huntsville, Huntsville AL 35899*

Abstract. The plasma spheroidization system (PSS) is the first process in the development of tungsten-uranium dioxide (W-UO_2) fuel cermets. The PSS process improves particle sphericity and surface morphology for coating by chemical vapor deposition (CVD) process. Angular fully dense particles melt in an argon-hydrogen plasma jet at between 32-36 kW, and become spherical due to surface tension. Surrogate CeO_2 powder was used in place of UO_2 for system and process parameter development. Particles range in size from 100 – 50 microns in diameter. Student's t-test and hypothesis testing of two proportions statistical methods were applied to characterize and compare the sphericity of pre and post process powders. Particle sphericity was determined by irregularity parameter. Processed powders show great than 800% increase in the number of spherical particles over the stock powder with the mean sphericity only mildly improved. It is recommended that powders be processed two-three times in order to reach the desired sphericity, and that process parameters be optimized for a more narrow particles size range.

Keywords: spherocity, spheroidization, plasma, uranium-dioxide, cermet, nuclear, propulsion

INTRODUCTION

Conventional chemical propulsion systems alone cannot provide the energy density and efficiency needed for successful long duration manned and robotic space flight missions; therefore new propulsion technologies must be leveraged if mankind is to continue pioneering the frontier of space. Nuclear fission type power generation and propulsion systems are a necessary evolution in realizing near term space exploration goals. NASA's MSFC is developing tungsten-uranium dioxide fissile fuel rod samples for solid-core nuclear thermal rocket (NTR) technology applying new manufacturing and material processing technologies to build on the success of Rover-NERVA research.

An NTR's solid core may be made of an arrangement of bundled hexagonal fuel rods[2]. These fuel rods are made of highly enriched UO_2 fuel powders encapsulated in Tungsten (W) to form a cermet (ceramic-metallic) matrix composite. During the 1960's and 1970's, the joint NASA and Atomic Energy Commission's (AEC) Rover-NERVA program spent extensive time on the development of graphite based composite fuels for NTR engines[10]. Subsequent efforts such as the ANL 200 and GE 710 programs went on to investigate W-UO_2 cermet fuel forms. Fissile fuel loss was an issue heavily researched with no simple solution. The prevalent theory, according to Haertling[5], was that UO_2 fissile fuel loss occurs due to mechanical failures of the fuel rod's tungsten cladding caused by formation of UH_3 resulting in large volumetric expansion. Hydrogen penetrates into the cermet matrix by bulk or grain boundary diffusion at high temperatures and reacts with the UO_2 producing oxygen deficient UO_2 as seen in Eq. (i). Upon cooling, substoichiometric UO_{2-x} dissociates releasing free U as seen in Eq. (ii).

$$UO_2 + xH_2 \rightarrow UO_{2-x} + xH_20 \quad \text{(i)}$$

$$2UO_{2-x} \rightarrow (2-x)UO_2 + xU \quad \text{(ii)}$$

$$2U + 3H_2 \leftrightarrow 2UH_3 \quad \text{(iii)}$$

The free uranium, which has a melting point well below the NTR core temperature, migrates along grain boundaries where it reacts with an excess of hydrogen and can form UH_3 within the cermet; Eq.(iii). Rover-NERVA era investigations found that fissile fuel loss could be mitigated through process control techniques to improve particle density and purity, particle packing density and particle surface morphology. Spherocity, density, purity, and surface morphology of UO_2 powder can be improved using thermal plasma processing.

EXPERIMENT DESIGN

The PSS is a 14 foot tall vertically oriented water cooled stainless steel vacuum chamber mounted inside of a carbon steel frame with a commercial spray plasma torch mounted inside the top of the chamber. A nearby control console manages the plasma forming gases, DC power supply for the plasma gun, and chamber vacuum level. Powder is metered and transported to the plasma gun by a commercial powder feeder. Operations require two operators.

The three 12 inch diameter 304 stainless steel (SS) pipe sections that compose the 100 inch long chamber have an internal volume of 7.5 cubic feet. The chamber segments are mated together with Flexitallic 347 SS spiral-wound gaskets between ANSI B16.5 class 150 series weld neck flanges. Each chamber segment has 304 SS sheets rolled and welded together on each chamber segment seated on the weld neck of the flanges leaving a sealed volume in which cooling water flows.

Figure 1. NASA MSFC UO_2 PSS

The Praxair model SG-100 multi-mode plasma spray gun is mounted on two brass feedthroughs that served as rigid mounts and supplied deionized cooling water to the anode, cathode, and gun face plate. The gun must be electrically isolated; therefore, the brass feedthroughs are mounted on a non-conductive garolite plate machined to mount to the PSS chambers top plate CF675-HN. Argon is the primary arc forming gas and a secondary gas of either hydrogen or helium was used to increase the heat content and velocity of the plasma. The SG-100 operates at maximum power level of 100 kW and must be water cooled[9]. The SG-100 is powered by a Halmer Robicon 120 kW power supply and a deionized water supply pump with reservoir supplies cooling water. The plasma gun starter current is provided by a Praxair HF-2000 high frequency starter box.

Figure 2. Praxair SG-100 setup

Stock powder and plasma-forming gases are routed to the SG-100 by 0.25 inch SS tubes inside of the chamber and 0.25 inch teflon tubes outside of the chamber. Powder can either be internally or externally injected into the plasma jet though external injectors mitigate the risk of powder clogging inside of the gun.

The top chamber segment (TCS) has two 600CF-HN (con-flat half nipples) clocked 90 degrees apart where Quartz viewports are fastened allowing the plasma torch to be viewed from two perspectives, which offer relevant operator based information about how the powder interacts with the plasma. The bottom chamber segment (BCS) reduces the chamber's internal diameter from 12 inches to 2 inches. The conical transition was machined from a single billet of 304 SS to a 30 degree half angle to allow the powders to efficiently flow towards the center and bottom of the chamber to be collected in a removable hopper. The transition matched the wall thickness of the 12 inch pipe segments. The reduced end of the transition is machined to accept a counter bored 450CF flange. An auxiliary threaded 304 SS coupling is welded onto the bottom of the BCS to allow the PSS chamber water jackets to be drained.

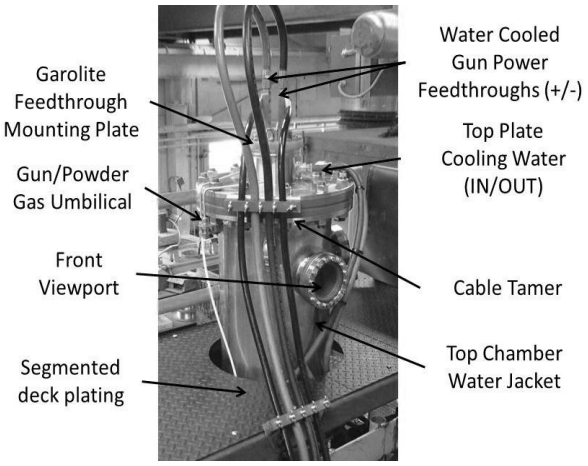

Figure 3. PSS Top Chamber Segment

The Effluent Gas Management System (EGMS) has an Edwards RV8 rotary vane pump, two custom designed ASME AG-1 compliant HEPA filter assemblies with pre-screens, a 1 inch Swagelok 0.334 psig relief valve, and a vacuum control valve. The EGMS mounts to the 600CF-NH on the middle chamber segment of the PSS. Chamber vacuum level is measures by analogue vacuum dial gauge. The vacuum level is controlled by a manual vacuum pump bypass valve. The PSS typically operates at 350 - 600 torr. Typical total gas flow into the chamber from the gun and powder feeder is 2 - 4 scfm. The flow rates of the plasma-forming gases are regulated by flow control orifices and upstream gas pressure[4].

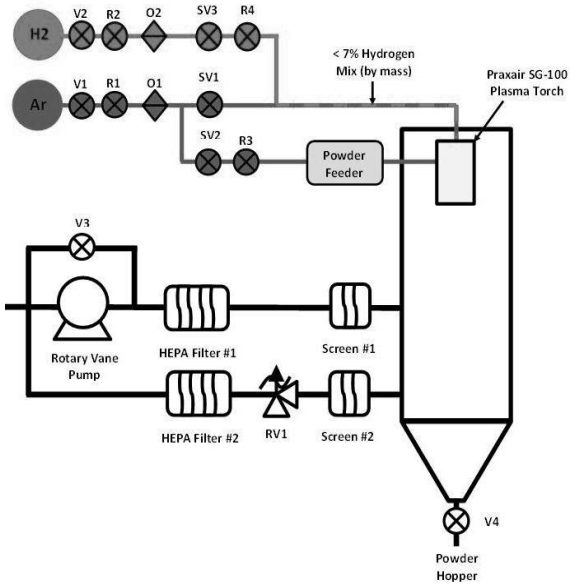

Figure 2. PSS EGMS Diagram

Surrogate powder spheroidization tests used the EPPI 171D powder feeder. The UO_2 spheroidization tests will use a rebuilt EPI 60C powder feeder. The powder feeder meters the powder into a carrier gas at 0.34 – 1.0 oz./min. The 60C powder hopper was modified to support a butterfly valve and quick flange on the top for isolated transfer of the UO_2 powders into the hopper. Three custom 2 lb. capacity powder transfer and loading hoppers were built to attach to the 60C as well as the bottom of the PSS for handling UO_2 safely.

RESULTS AND DISCUSSION

The purpose of the PSS is to improve the spherocity of UO_2 powder by plasma processing. Simultaneously, surface morphology should be improved making the particles a better substrate for CVD coating. In theory, angular powder is transported through a plasma jet by a carrier gas, where the powder is melted in the plasma jet. The particle consolidates and becomes spherical due to surface tension. Undesired trace elements are vaporized in the plasma flame yielding a higher purity product. The particle solidifies as it exits the plasma jet. The result is a highly dense, pure, and spherical particle with ideal surface morphology for coating[1].

These experiments used F. J. Brodmann & Co. L.L.C. manufactured Cerium Oxide (CeO_2) as a surrogate for UO_2. CeO_2 melts at 2673 K, which is lower than the melting point of UO_2 at 3138 K, but has a phase composition that closely matches that of UO_2, hence the motivation for developing CeO_2 spheroidization parameters and process controls. The Brodmann CeO_2 powder is angular, fully dense, sintered, and crushed powder that is more like the stock UO_2 powders that will be received from Idaho National Laboratories (INL) for W-UO_2 cermet fuel development. The powder was classified into ranges (63-75microns, 75-90 microns, and 90-106 microns) and photographed by a LEICA stereomicroscope like that illustrated in Figure 5.

Figure 3. Stock Brodmann CeO_2 (75-90 micron)

Statistical inference between the population and the samples is established by first assuming that the data is normally distributed, that there exists an equality of variance between the population and the powder sample, and that sample particle's data is independent of others. It is therefore possible to apply the Central Limit Theorem[6]. 50 particles were randomly selected from each range and evaluated for minimum circumscribed diameter (d_1), maximum inscribed diameter (d_2), evidence of shelling and/or agglomeration, color, and surface morphology. The particles mean diameter was calculated using Eq. (1), and the particle's spherocity was calculated using the irregularity parameter (IP_i) in Eq. (2)[4]. The sample's mean particle size (d_{avg}) and irregularity parameter ($\overline{IP}$) may be calculated using Eq. (3), and the standard deviation for mean diameter (s_d)and irregularity parameter (s_{IP}) may be calculated using Eq. (4). Utilizing Student's t-distribution testing[6], and accepting an $\overline{IP} \leq 1.2$ as the criteria for spherocity[8], it was shown that the stock Brodmann CeO_2 powder is not spherical and that it is a very low probability that it is by chance; Table 1. Now, the goal of the PSS runs is to improve the spherocity of the CeO_2 powder and to do so with a low probability that it is by chance.

Table 1. Summary of Stock Brodmann CeO2 Statistical Analysis

PSS Run #, Powder Type, Size Range	IP_{avg} [StDev]	t_{calc}	t_{crit}	Prop	C.I. (95%)
Stock; Brodmann CeO2; 90µm-106µm	1.49 [0.22]	9.195	1.676	0.01%	1.421 - 1.544
Stock; Brodmann CeO2; 75µm-90µm	1.53 [0.21]	11.302	1.676	0.01%	1.464 - 1.578
Stock; Brodmann CeO2; 63µm-75µm	1.51 [0.22]	10.195	1.676	0.01%	1.447 - 1.567

PSS runs #8 and #9 were conducted on 10 Oct 2012, and were the first to process fully dense and angular powders. Figure 6 shows the PSS in operation. The powder can be seen entrained in the plasma clearly near the bottom of the jet. The process parameters used for Runs #8 and #9 where referenced from recommended operational parameters for processing similar powders[9] and are listed in Table 2.

Table 2. PSS processing parameters

Run	Power (kW)	Current (Amps)	Vacuum (Torr)	Arc Gas	Flow Rate (SCFM)
8	32.8	820	400	Ar-H_2	105
9	36.9	820	760	Ar-H_2	105

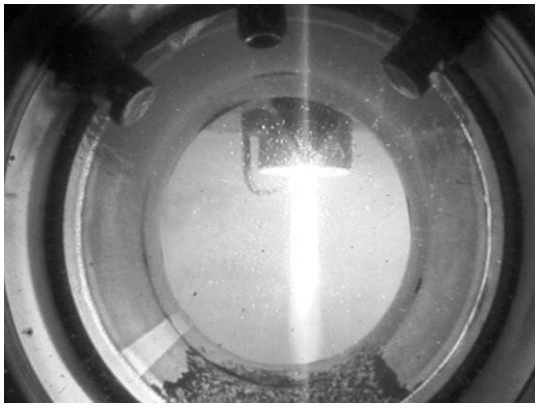

Figure 4. PSS in operation

The Run #8 and #9 powders were separately classified into three ranges (63-75 microns, 75-90 microns, and 90-106 microns) and a sample was prepared for each range for imaging. Run #8 and #9 powders were progressively darker as particle size decreases as shown in Figure 7. This observation may be evidence of dissociation, which may indicate that the powders were processed a too high a temperature. It is believed that the darkening is only on the surface and due to oxidation of the free cerium, but further analysis is needed to determine the nature of the darkening of processed particles. As with the stock Brodmann powders, 50 randomly selected particles from each range were evaluated for minimum circumscribed diameter (d_1), maximum inscribed diameter (d_2), evidence of shelling or agglomeration, color, and surface morphology.

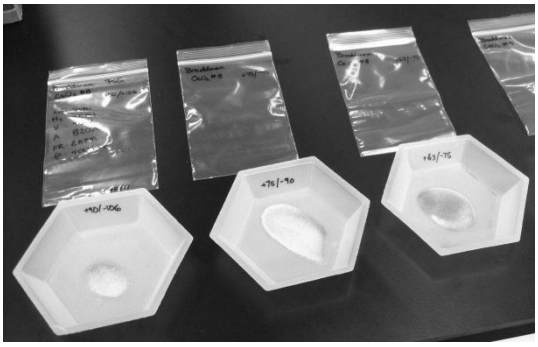

Figure 5. Sieve Run #8 powders before imaging

Hypothesis testing of two-proportion[6] showed that the Run #8 and #9 powders exhibited a statistically significant improvement in spherocity. It was also observed that while the powders are more spherical after processing, the mean irregularity parameters for the run #8 and #9 powders exceeded the desired maximum of 1.2. This observation is supported by applying the same statistical method utilized to characterize the stock Brodmann powders. The Run #8 and #9 powders are also not spherical according to the established criteria; but are significantly closer; Table 3.

Table 3. PSS Run #8 and #9 Statistical Data

PSS Run #, Powder Type, Size Range	IP_{avg} [StDev]	Spherical	Z_{calc}	Z_{crit}	Prop	C.I. (95%)
Run #8; Brodmann CeO2; 90µm-106µm	1.2 [0.21]	66%	-5.769	1.645	< 0.01%	1.136 - 1.253
Run #8; Brodmann CeO2; 75µm-90µm	1.39 [0.29]	32%	-3.993	1.645	< 0.01%	1.305 - 1.465
Run #8; Brodmann CeO2; 63µm-75µm	1.37 [0.24]	28%	-3.641	1.645	< 0.01%	1.297 - 1.429
Run #9; Brodmann CeO2; 90µm-106µm	1.3 [0.18]	30%	-2.73	1.645	< 0.33 %	1.243 - 1.345
Run #9; Brodmann CeO2; 75µm-90µm	1.29 [0.2]	34%	-4.165	1.645	< 0.01 %	1.233 - 1.343
Run #9; Brodmann CeO2; 63µm-75µm	1.34 [0.3]	38%	-4.500	1.645	< 0.01 %	1.249 - 1.415

The Run #8 Brodmann CeO_2 powder processed at 32.8 kW in argon-hydrogen plasma showed significant improvement with 42% of the particles passing as spherical (compared to <5% of stock) and the mean IP was improved from 1.51 to 1.32, which is a 60% improvement, but it is still above the desired mean IP. Also, 40% of the powder was noted as having a good surface morphology for coating. The Run #9 Brodmann CeO_2 powder was processed at 36.9 kW in argon-hydrogen plasma and did not show as significant an improvement as Run #8 with 34% of the particles passing as spherical, but the mean IP was slightly more improved from 1.51 to 1.31, which is a 65% improvement, but it is still above the desired mean IP. Nearly 60% of the powder was noted as having a good surface morphology.

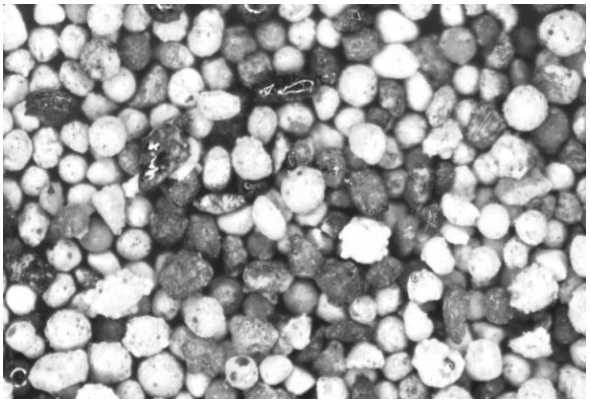

Figure 6. PSS Run #8 CeO_2 (90-106 microns)

CONCLUSIONS

The PSS successfully improved the spherocity of angular stock CeO_2 surrogate powder The Run #8 Brodmann CeO_2 powder was processed at 32.8 kW in argon-hydrogen plasma and showed significant improvement with 42% of the particles passing as spherical (compared to <5% of stock) and the mean IP was improved from 1.51 to 1.32. The Run #9 Brodmann CeO_2 powder was processed at 36.9 kW in argon-hydrogen plasma and did not show as significant an improvement as Run #8 with 34% of the particles passing as spherical. It is evident that the operational parameter for run #8 and #9 will not yield the desired spherocity of the surrogate powders in one pass. Multiple passes through the PSS would be required to lower the mean IP to below 1.2 and further improve the surface morphology. Further development is needed to optimize spheroidization parameters.

ACKNOWLEDGMENTS

I would like to thank the NASA Marshall Space Flight Center personnel who were involved in the fabrication of the PSS hardware: Keith Chavers, Ronnie Renfroe, Bart Suggs, and Roger Harper. Thank you to Robert Hickman, Jeramie Broadway, and Omar Mireles for assigning me to this project.

REFERENCES

[1] Ananthapadmanabhan, P. V., "Chapter 6: Thermal plasma processing." in *Pergamon Materials Series*, 1999, Vol. 2, pp. 121-150.
[2] Angelo, J. A., *Space Nuclear Power*, Malabar, FL: Orbit Book Company, Inc., 1985.
[3] Cochran, *Final report for FY 1965 on Tungsten-Uranium dioxide Materials for NASA: Oak Ridge National Laboratory*, 1965.
[4] Crane Co., *Flow of fluids through valves, fittings, and pipe*. Chicago: Crane Co., 1957.
[5] Haertling, C., *Literature review of thermal and radiation performance parameters for high-temperature, uranium dioxide fueled cermet materials.* Journal of Nuclear Materials, 2007, 366(3), 317-335.
[6] Holman, J. P. (2001). *Experimental methods for engineers*. Boston: McGraw-Hill.
[7] Károly, Z., *Plasma spheroidization of ceramic particles. Chemical Engineering and Processing: Process Intensification*, 2005, 44(2), 221-224.
[8] Kumar, S., "Spheroidization of metal and ceramic powders in thermal plasma jet" in *Computational Materials Science*, 2006, 36(4), 451-456.
[9] Praxair Surface Technologies, Inc., *Model SG-100 Plasma Spray Gun Operator's Manual*, 2010.
[10] Saunders, N. T., *Feasibility study of a Tungsten Water-Moderated Nuclear Rocket II. Fueled Materials: NASA Lewis Research Center*, 1968.

EQUATIONS

$$\bar{d}_i = {d_{1,i} + d_{2,i}}/{2} \tag{1}$$

$$IP_i = {d_{1,i}}/{d_{2,i}} \tag{2}$$

$$\bar{x} = \frac{1}{n}\sum x_i \tag{3}$$

$$s_x = \sqrt{\Sigma(x_i - \bar{x})^2/(n-1)} \tag{4}$$

$$H_0 \leq 1.2 \tag{5}$$

$$H_A > 1.2 \tag{6}$$

$$t_{calc} = {(\overline{IP} - \mu_0)}/{\left(s/\sqrt{n}\right)} \tag{7}$$

$$C.I. = \bar{x} \pm t_{(1-\alpha/2,DOF)} \times {s}/{\sqrt{n}} \tag{8}$$

$$H_0: \hat{p}_{stock} \geq \hat{p}_{Run\#8} \text{ or } \hat{p}_{stock} - \hat{p}_{Run\#8} \geq 0 \tag{9}$$

$$H_A: \hat{p}_{stock} < \hat{p}_{Run\#8} \text{ or } \hat{p}_{stock} - \hat{p}_{Run\#8} < 0 \tag{10}$$

$$\bar{p} = \frac{x_1 + x_2}{n_1 + n_2} \tag{11}$$

$$\bar{q} = 1 - \bar{p} \tag{12}$$

$$z = \frac{(\hat{p}_1 - \hat{p}_2)}{\sqrt{\frac{\bar{p}(1-\bar{p})}{n_1} + \frac{\bar{p}(1-\bar{p})}{n_2}}} \tag{13}$$